

Maximum Efficiency Tracking of Underwater Wireless Power Transmission System Based on Dynamic Coupling Coefficient Estimation

Zhongjiu Zheng, Yanpeng Ma*, Xingfeng Cao, Zhilong Wu, and Jinjun Bai

College of Marine Electrical Engineering, Dalian Maritime University, Dalian 116026, China

ABSTRACT: For the complex marine environment, the water flow disturbance causes the receiver offset, which leads to the decrease of mutual inductance and the decrease of system efficiency. This paper proposes an estimation method of dynamic coupling coefficient without communication and further realizes the maximum efficiency point tracking (MEPT) on the receiving side. By collecting the effective value of the fundamental current on the receiving side, the equivalent impedance mode equation of mutual inductance is established, and the mutual inductance is identified in real time by numerical solution method. On the basis of the identification results, the impedance matching is realized by the closed-loop controller designed on the receiving side, and the maximum efficiency point tracking of the system is realized. In this paper, the experimental platform is built, and the effectiveness of the method is verified by experiments. The experimental results show that the accuracy of mutual inductance estimation is more than 95%, and the efficiency of the system is improved by 18% after using the maximum efficiency point tracking.

1. INTRODUCTION

Underwater electromechanical equipment has shown very important application value in the fields of marine exploration, ocean development, and hydrological monitoring. As the main power source of underwater electromechanical equipment, the transmission mode of electric energy has become a major problem. The traditional underwater power transmission mainly adopts the wet insertion method, and the power is transmitted through the metal wire. The underwater environment will lead to corrosion and aging of metal wires, shorten the service life, and this wet plug interface has many disadvantages such as complex docking, high cost, and short service life. Refs. [1–4] mentioned that wireless power transmission (WPT) technology has gradually replaced some traditional power supply methods with the advantages of low maintenance cost, high reliability, and good waterproof. In [5, 6], it is further mentioned that underwater wireless power transmission can effectively avoid the problems in traditional methods, such as the vulnerability of wired charging to seawater corrosion. However, when working in an underwater environment, due to the influence of water flow factors, underwater electromechanical equipment cannot remain stationary like land-based equipment, which leads to the deviation of the coupling mechanism during underwater charging. When the receiving coil deviates from the transmitting coil, the mutual inductance of the system will decrease, which will lead to a decrease in the efficiency of the system and a sharp increase in power loss.

In order to improve the transmission efficiency of WPT systems under offset conditions, scholars have conducted a lot of

research work. Ref. [7] introduces the factors that affect transmission efficiency. When the system parameters are constant, dynamic changes in mutual inductance and load can cause fluctuations in system transmission efficiency. If the load and mutual inductance values are known, there will be multiple methods applicable to improving system efficiency. Therefore, how to accurately estimate mutual inductance and load value, as well as mutual inductance, is highly valued by everyone.

For the estimation of the load, [8] proposes a transient model of the series-series compensated WPT system to detect the initial load condition by injecting a series of high-frequency signals before starting. However, it does not track real-time changes in load. By adjusting its operating frequency and measuring the output voltage and current of the inverter, [9] can realize parameter identification of the system mutual inductance and load without communication, and the identification error is within 7%. Ref. [10] proposes a new impedance spectrum analysis method. By making the system not work at the resonant frequency, the system working information at different frequencies can be obtained, and the system load and mutual inductance can be estimated without measuring the receiving side. However, these methods need to adjust the operating frequency of the system frequently, which will have an impact on its work efficiency. In [11], by using the Bluetooth module to receive the current information of the transmitting end, the equivalent impedance of the receiving end is changed, and the MPET based on the best load matching is realized. On this basis, the constant voltage output of the system is realized. This method can keep the system efficiency at about 50% when the receiver is offset by 60 mm.

* Corresponding author: Yanpeng Ma (m2802269239@dlmu.edu.cn).

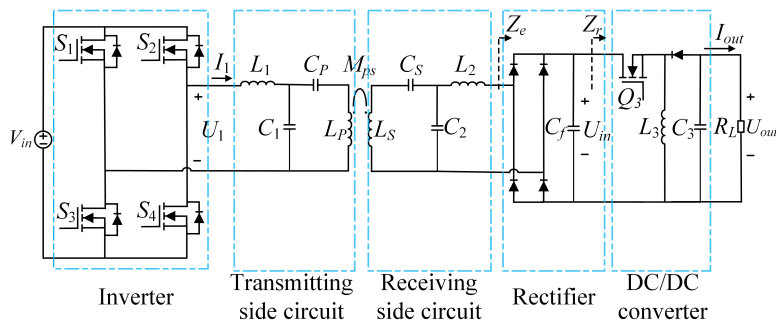


FIGURE 1. DLCC compensated WPT system structure.

Coupling coefficient estimation refers to the use of relevant methods to obtain the mutual inductance between the transmitting coil and receiving coil, and to estimate it by using known electrical quantities or control algorithms [12–16]. In [17], a wireless power transmission system based on harmonic information is proposed. By using harmonic and band-stop filtering, the mutual inductance is estimated, and the maximum efficiency tracking of the system is further realized. Ref. [18] proposes that the mutual inductance of the static receiver can be estimated only by using the electrical quantity of the transmitting side without the secondary side information. This method obtains the required information by measuring the amplitude and phase difference of the input voltage and the input current, and then solves it. The mutual inductance and load can be estimated. Ref. [19] proposes to use an amount of information on the transmitting side to dynamically estimate the mutual inductance coupling through the dual impedance mode constraint. In [20], an approximate real-time mutual inductance identification method is proposed. The mutual inductance value is estimated by measuring the voltage on the transmitting side and the voltage and current on the receiving side, and the maximum efficiency tracking is performed. However, this method requires bilateral communication, but bilateral communication always encounters some headaches: wireless communication modules increase additional hardware and software costs. Strong magnetic field interference may affect the stability of communication, and some specific applications are not suitable for wireless communication, such as underwater and aerospace. Therefore, how to realize the MPET of WPT system by identifying the coupling coefficient in real time without communication has been accepted as an important solution by academia and industry.

In the process of underwater charging, the receiver is more prone to offset than the load change, so this paper focuses on the identification of mutual inductance. Therefore, under the assumption that the load is constant, this paper proposes an identification method based on the mutual inductance of the system based on the electrical quantity of the receiving side. Compared with the current research, the contributions of this paper are as follows:

1) A new method for dynamic identification of mutual inductance has been proposed, which does not require bilateral communication and only utilizes the effective value of the current flowing through the receiving side to achieve mutual induc-

tance identification. The process of mutual inductance identification results has been analyzed in detail.

2) A Maximum Efficiency Point Tracking method based on dynamic coupling coefficient estimation is proposed. This method is applied to the receiving end, which reduces the requirements of the system on the transmitting end and contributes to the application of the receiver on different transmitting platforms.

The organizational structure of this paper is as follows. In the second Section, the mathematical model of double side inductor capacitor capacitor (DLCC) topology WPT system is established, and the influence of equivalent load and mutual inductance on system efficiency is analyzed. Section 3 introduces the receiving side control. Section 4 verifies the feasibility of the method through experiments. Finally, the Section 5 summarizes the conclusions of the full text.

2. MODELING AND ANALYSIS OF DLCC SYSTEM

2.1. System Efficiency Analysis

In the current research, four basic resonant topologies have been widely used. However, only the resonant frequency of the S - S topology is independent of the mutual inductance [22]. In recent years, high-order resonant circuits such as inductor capacitor inductor (LCL) and inductor capacitor capacitor (LCC) have also been adopted. The LCC topology has the characteristics that the primary coil current is not affected by load and mutual inductance, and has certain advantages in the calculation simplification of the coupling coefficient estimation method, which is more suitable for underwater wireless power transmission. Therefore, DLCC topology is selected in this paper. The system structure is composed of high-frequency inverter bridge, transmitting mechanism and receiving mechanism, rectifier, DC/DC converter and load, as shown in Fig. 1.

In Fig. 1, V_{in} is the DC voltage source, and the high-frequency inverter bridge contains four MOSFETs S_1 - S_4 . The primary and secondary side compensation network consists of compensation inductance L_1 , L_2 , and compensation capacitance C_1 , C_2 , C_s , C_p . The DC/DC part is composed of switch Q_3 , inductor L_3 , and output capacitor C_3 , and the load resistance is R_L . In order to facilitate subsequent calculations, the equivalent circuit shown in Fig. 2 is obtained.

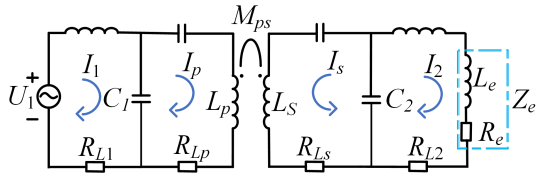


FIGURE 2. Equivalent circuit of DLCC WPT system.

In Fig. 2, the input voltage U_1 is the equivalent AC power supply, which is equivalent to the DC power supply and inverter, and its value is shown by Formula (1).

R_{L1} , R_{Lp} , R_{Ls} , and R_{L2} are the compensation inductance and internal resistance of the coil, and M_{ps} is the mutual inductance between the receiving coil and transmitting coil. The equivalent load of the system can be expressed as $Z_e = R_e + jX_{Le}$, where $X_{Le} = \omega L_e$. The specific expressions of the equivalent inductance L_e and equivalent resistance R_e are shown in Formula (2):

$$U_1 = \frac{2\sqrt{2}}{\pi} V_{in} \sin \frac{\alpha}{2} \quad (1)$$

$$\begin{cases} R_e = \frac{8\omega^2 L_2^2 R_L}{(\pi - \frac{8}{\pi})^2 R_L^2 + \pi^2 \omega^2 L_2^2} \\ L_e = \frac{8(1 - \frac{8}{\pi^2}) L_2 R_L^2}{(\pi - \frac{8}{\pi})^2 R_L^2 + \pi^2 \omega^2 L_2^2} \end{cases} \quad (2)$$

where α is the conduction angle of the inverter.

Starting from the equivalent circuit of Fig. 2, I_4 , I_p , I_s , I_1 are the effective values of each loop current, and according to [21] can be written in the circuit equation of each current loop.

$$\begin{cases} \dot{I}_1 \left(j\omega L_1 + \frac{1}{j\omega C_1} + R_{L1} \right) - \dot{I}_p \frac{1}{j\omega C_1} = \dot{U}_1 \\ \dot{I}_p \left(j\omega L_p + \frac{1}{j\omega C_1} + \frac{1}{j\omega C_p} + R_{Lp} \right) - \dot{I}_1 \frac{1}{j\omega C_1} \\ = -j\omega M_{ps} \dot{I}_s \\ -\dot{I}_s \left(j\omega L_s + \frac{1}{j\omega C_2} + \frac{1}{j\omega C_s} + R_{Ls} \right) - \dot{I}_2 \frac{1}{j\omega C_2} \\ = j\omega M_{ps} \dot{I}_p \\ \dot{I}_2 \left(j\omega L_2 + \frac{1}{j\omega C_2} + R_{L2} + Z_e \right) + \dot{I}_s \frac{1}{j\omega C_2} = 0 \end{cases} \quad (3)$$

Among them, \dot{U}_1 is the phasor of the input voltage; I_4 , I_p , I_s , I_1 are the current phasors of each loop; ω is the angular frequency of the system, which satisfies $\omega = 2\pi f$.

According to [19], the angular frequency under resonant conditions is shown in Formula (4):

$$\begin{aligned} \omega &= \frac{1}{\sqrt{L_1 C_1}} = \frac{1}{\sqrt{L_2 C_2}} = \frac{1}{\sqrt{(L_p - L_1) C_p}} \\ &= \frac{1}{\sqrt{(L_s - L_2) C_s}} \end{aligned} \quad (4)$$

Simplify the calculation, and ignore the parasitic resistance R_{L1} , R_{L2} of the primary and secondary compensation inductance. According to Formula (4), the output power and input

power of the system can be calculated as:

$$\begin{cases} P_{in} = \dot{U}_1 \dot{I}_1 = \left(\omega^2 C_1^2 R_{Lp} + \frac{\omega^6 M_{ps}^2 C_1^2 C_2^2 Z_e}{1 + \omega^2 Z_e R_{Ls} C_2^2} \right) U_1^2 \\ P_{out} = |\dot{I}_2|^2 Z_e = \frac{\omega^6 M_{ps}^2 C_1^2 C_2^2 Z_e}{(1 + \omega^2 Z_e R_{Ls} C_2^2)^2} U_1^2 \end{cases} \quad (5)$$

Further, the efficiency of the inverter fundamental output to the load is

$$\eta = \frac{\omega^4 M_{ps}^2 C_2^2 Z_e}{(\omega^2 Z_e C_2^2 R_{Ls} + 1) (\omega^2 Z_e C_2^2 (R_{Ls} R_{Lp} + \omega^2 M_{ps}^2) + R_{Lp})} \quad (6)$$

Generally, the inductance resistance of the resonant coil, the internal resistance of the compensation capacitor, and the resonant frequency are considered to be constant. Therefore, in the WPT system, the system efficiency is mainly determined by M_{ps} and Z_e . The underwater environment is easy to cause the receiver to shift, which will lead to a decrease in mutual inductance. It can be seen from Formula (6) that as the mutual inductance decreases, the efficiency of the system also decreases. However, when the load changes, the system efficiency may increase or decrease, depending on whether the resistance reaches the optimal equivalent load.

The derivative of Formula (6) is obtained, and the value of the equivalent load when the system transmission efficiency is the highest Z_{opt} is

$$Z_{opt} = \frac{1}{\omega^2 C_2^2} \sqrt{\frac{R_{Lp}}{(\omega^2 M_{ps}^2 + R_{Lp} R_{Ls}) R_{Ls}}} \quad (7)$$

It can be seen from Formula (7) that when the system parameters are constant, Z_{opt} is only related to mutual inductance. Once the mutual inductance is estimated, the optimal equivalent resistance can be calculated. Therefore, it is necessary to carry out real-time mutual inductance, and on this basis, further adjust the equivalent load of the system to achieve efficient operation of the system.

3. RECEIVING SIDE CONTROL

3.1. Impedance Matching for Maximum Efficiency Tracking

When the system works at the maximum efficiency point, the optimal load value Z_{opt} can be calculated by Formula (7). In this paper, the equivalent impedance Z_e is adjusted by changing the duty cycle of the Buck-Boost converter. When Z_e is equal to Z_{opt} shown in Formula (7), the maximum efficiency transfer of the system can be achieved.

Assuming that the Buck-Boost converter works in continuous current mode (CCM), the duty cycle should meet the following requirements:

$$D \geq 1 - \frac{\sqrt{2L_3 R_L f_2}}{R_L} \quad (8)$$

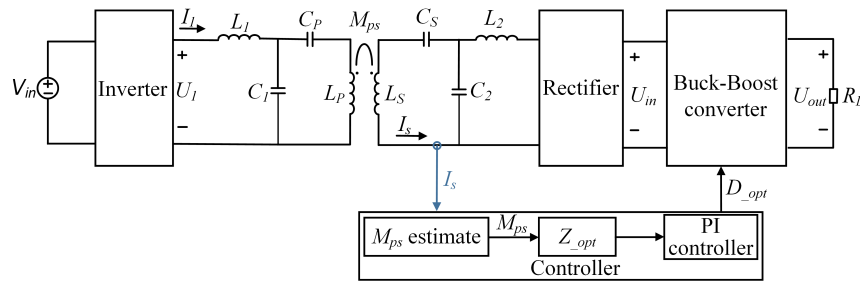


FIGURE 3. Control chart of WPT system with MEPT.

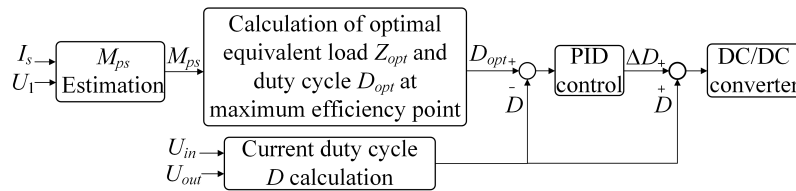


FIGURE 4. Tracking process flow chart.

Among them, f_2 is the frequency of the switch in the Buck-Boost converter. Assuming that the Buck-Boost converter operates in ideal mode without power loss, the relationship between the output voltage and input voltage is given by Formula (9), and the relationship between the equivalent input resistance Z_r and load R_L is given by Formula (10).

$$U_{out} = \frac{D}{1-D} U_{in} \quad (9)$$

$$Z_r = \left(\frac{1-D}{D} \right)^2 R_L \quad (10)$$

Similarly, the relationship 1 between the equivalent load resistance Z_e and equivalent input resistance Z_r is as follows:

$$Z_e = \frac{8}{\pi^2} Z_r \quad (11)$$

The duty cycle D of the current DC/DC converter can be obtained from Formula (9).

$$D_{opt} = 1 / \left(1 + \sqrt{\frac{\pi^2 Z_{opt}}{8R_L}} \right) \quad (12)$$

At this point, in order to achieve the tracking of the optimal duty cycle, this paper designs a closed-loop controller to adjust the duty cycle of the Buck-Boost converter in real time to achieve impedance matching. The WPT system control diagram is shown in Fig. 3. This method does not require communication. On the secondary side, two steps are required to complete the maximum efficiency tracking.

1) By measuring the current flowing through the receiving coil \dot{I}_s , the mutual inductance of the current working state is estimated.

2) The optimal duty cycle D_{opt} of Buck-Boost converter is calculated by Formula (12).

A detailed flowchart of the MEPT method is shown in Fig. 4. Firstly, the current information of the receiving end is extracted, and the parameters of the mutual inductance are identified. The identification process will be introduced in Section 3.2. Then, the obtained mutual inductance estimation value is brought into Formula (7) to calculate the optimal equivalent load value Z_{opt} of the current system. Finally, based on the optimal equivalent load Z_{opt} , the optimal duty cycle D_{opt} is calculated according to Formula (12), and the maximum efficiency tracking of the dynamic WPT system can be realized.

3.2. Mutual Inductance Dynamic Estimation

Starting from Formula (6), the efficiency of the system is affected by the mutual inductance value. Therefore, in order to calculate the optimal equivalent impedance, the mutual inductance value is estimated, and the maximum efficiency tracking of the system is realized. The mutual inductance under different offset distances is measured on the experimental platform, and the variation curve of the coupling coefficient with the offset distance is obtained as shown in Fig. 5. With the increase of offset distance, the coupling coefficient of the system is not a fixed value. Therefore, it needs to be accurately estimated.

For the real-time estimation of mutual inductance, this paper starts from the equivalent circuit of Fig. 6, the equivalent impedances Z_{c2} , Z_s , Z_r , Z_p , Z_c , Z_{in} are derived from [19].

According to Kirchhoff's law, the relationship between currents \dot{I}_p and \dot{I}_s is Formula (13).

$$0 = j\omega M_{ps} \dot{I}_p + Z_s \dot{I}_s \quad (13)$$

The relationship between voltages \dot{U}_{c1} and \dot{I}_p , \dot{I}_1 is shown in Formula (14) and Formula (15), respectively. Formula (16)

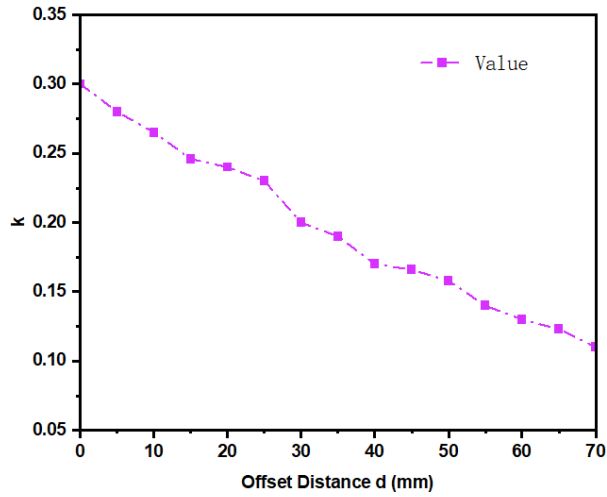


FIGURE 5. The relationship between coupling coefficient and offset distance.

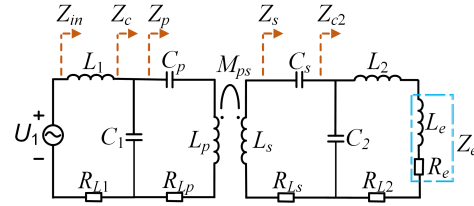


FIGURE 6. Equivalent circuit of DLCC type WPT system.

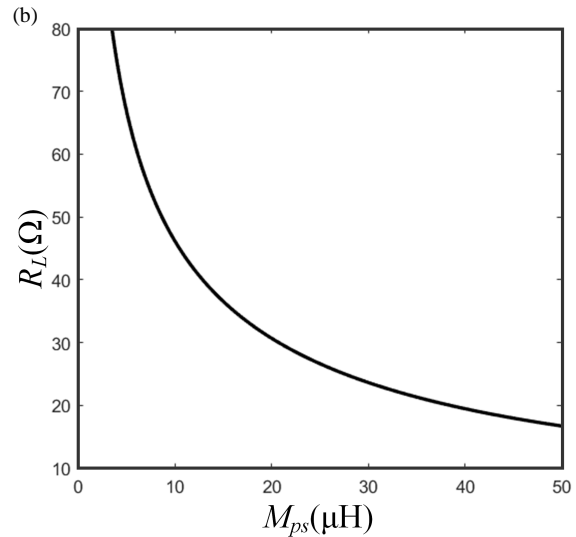
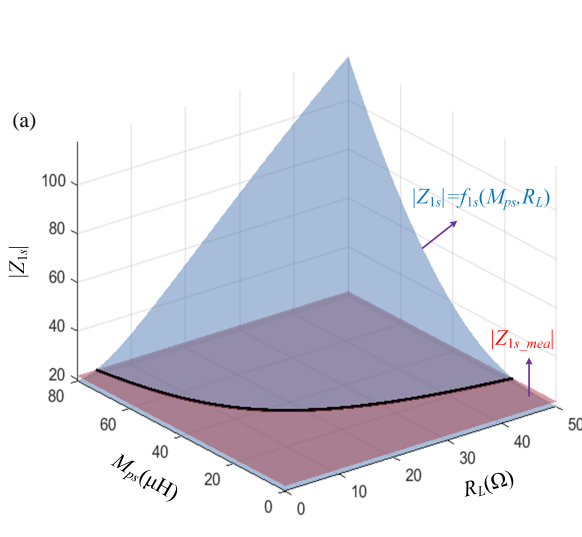


FIGURE 7. The relationship between $|Z_{1s}|$ and $|Z_{1s_meal}|$ and M_{ps} and R_L . (a) The three-dimensional graph under the constraint of $|Z_{1s_meal}| = 21.35$. (b) The top view under the constraint of $|Z_{1s_meal}| = 21.35$.

shows relationship between \dot{U}_1 and \dot{I}_1 .

$$Z_p = \dot{U}_{c1} / \dot{I}_p \quad (14)$$

$$\dot{U}_{c1} = \dot{I}_1 Z_c \quad (15)$$

$$\dot{I}_1 = \dot{U}_1 / Z_{in} \quad (16)$$

In summary, the relationship between \dot{U}_1 and \dot{I}_s is shown in Formula (17)

$$\frac{\dot{U}_1}{j\dot{I}_s} = \frac{Z_s Z_p Z_{in}}{Z_c \omega M_{ps}} \quad (17)$$

Let $Z_{1s} = \dot{U}_1 / j\dot{I}_s$, then $|Z_{1s}|$ and mutual inductance M_{ps} satisfy the functional relationship shown in Formula (18), where $|Z_{1s}|$ is the impedance Z_{1s} modulus value

$$|Z_{1s}| = f_{1s}(M_{ps}) = \left| \frac{Z_s Z_p Z_{in}}{Z_c \omega M_{ps}} \right| = \frac{|Z_s| |Z_p| |Z_{in}|}{\omega M_{ps} |Z_c|} \quad (18)$$

Based on the measured current flowing through the receiving coil I_{s_meal} , the impedance modulus of Z_{1s} can be calculated as shown in Formula (19):

$$|Z_{1s_meal}| = U_1 / I_{s_meal} \quad (19)$$

As shown in Fig. 7(a), the blue surface is the variation trend of $|Z_{1s}|$ with R_L and M_{ps} according to Formula (18). It should be noted that all the analysis processes in this paper are based on the system parameters corresponding to Table 1. The red plane is the measured value of the working point $(M_{ps}, R_L) = (43.5 \mu\text{H}, 30 \Omega)$.

As can be seen from Fig. 7(a), there is an intersection line between the red plane and blue surface, which is projected onto the XOY plane, as shown in Fig. 7(b). Fig. 7(b) shows that when the load or mutual inductance is fixed, each point (M_{ps}, R_L) on the intersection line can be substituted into For-

mula (18) to have a unique solution. Therefore, Formula (18) can be used to identify the system parameters.

According to the above analysis, the mutual inductance between the transmitting coil and receiving coil can be estimated according to the following steps.

- 1) Step 1: The effective value of the measured current \dot{I}_s is I_{s_mea} ;
- 2) Step 2: Calculate the measured value $|Z_{1s_mea}|$ according to Formula (19);
- 3) Step 3: Bring Z_s, Z_p, Z_c, Z_{in} into Formula (18);
- 4) Step 4: Calculate the mutual inductance M according to Formula (18).

4. EXPERIMENTAL VERIFICATION

In order to verify the accuracy of the mutual inductance estimation and the effectiveness of the maximum efficiency tracking control in the WPT system, the experimental verification is carried out on the experimental platform shown in Fig. 8. The experimental parameters used are shown in Table 1, in which the parameters of the compensation network components are accurately measured by the LCR Meter TL2812D. The experimental platform includes DC power supply, single-phase bridge inverter, DSP control unit (TMS320F28335), primary and secondary compensation network, uncontrolled rectifier bridge, electronic load, sampling circuit, DC/DC circuit, transmitting coil, and receiving coil. The transmitting coil and receiving coil are composed of a circular coil wound by the same excitation line. The inner diameter of the coil is 7.3 cm; the outer diameter is 22.3 cm; and the coil has 27 turns. The vertical distance between the two coils is 15 cm, that is, when the coil is facing, the mutual inductance is 43.5 μH . The sampling circuit is composed of a Hall current sensor and ADC chip (AD637).

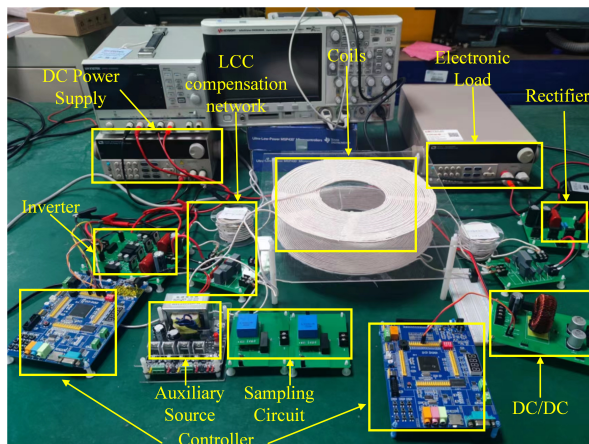


FIGURE 8. Experimental platform.

4.1. Coefficient Estimation Experiment

In order to evaluate the accuracy of Formula (18), it is verified by experiments. The mutual inductance estimation results are shown in Fig. 9. In Fig. 9(a), the line chart represents the mutual inductance estimation curve. The abscissa represents the true value of mutual inductance, and the ordinate represents the

TABLE 1. Experimental parameters.

Parameter	Value
L_p	145 μH
L_s	145 μH
L_1	33 μH
L_2	47 μH
L_{p1s}	145 μH
C_p	32.2 nF
C_1	106.94 nF
V_{in}	12 V
R_{lp}	109 m Ω
R_{ls}	100 m Ω
R_{l1}	66 m Ω
R_{l2}	91 m Ω
R_l	30 Ω
C_s	35.646 nF
C_2	74.795 nF
f	85 kHz

mutual inductance value estimated by the method in this paper. It can be seen that when the receiving coil is offset, the mutual inductance estimation value matches well with the real value. In order to further verify the matching, the estimation error is shown in Fig. 9(b). In Fig. 9(b), it can be seen that the overall error of the system is controlled within 4%, and the error may be caused by the measurement error of some electrical parameters, such as the inductance value of the coil and the inductance value and capacitance value of the compensation network. At the same time, the measurement deviation of WPT primary side electrical may also be one of the reasons, so the parameter identification method has good accuracy in the case of coil offset. Therefore, the experimental results further verify the accuracy of the estimation Formula (18) and prove the effectiveness of the proposed mutual inductance estimation method in the WPT system.

Figure 10 shows the dynamic shift of the coil, that is, the I_s change waveform when the coupling coefficient changes from 0.293 to 0.127. It can be seen from the figure that as the coupling coefficient changes, the current at the receiving end of the system changes. This paper can estimate the coupling coefficient according to the real-time changing current.

4.2. MEPT Experimental Results

In order to verify the effectiveness of the maximum efficiency tracking, the following experiments will be carried out. Firstly, the maximum efficiency tracking of coil offset and load change is studied. Secondly, a comparative study was conducted on whether to use the MEPT method. The results are as follows. Among them, the current waveform of this experiment is measured by oscilloscope current clamp, and the conversion ratio is 1 V voltage corresponding to 100 mA current.

For the mutual inductance disturbance, this paper fixes the load resistance to 30 Ω and makes the coil shift, that is, the coupling coefficient changes from 0.296 to 0.273. The system load voltage U_{out} and current I_{out} are collected, and the voltage and current change waveforms are shown in Fig. 11. It can be seen from the diagram that as the receiving side moves, the mutual

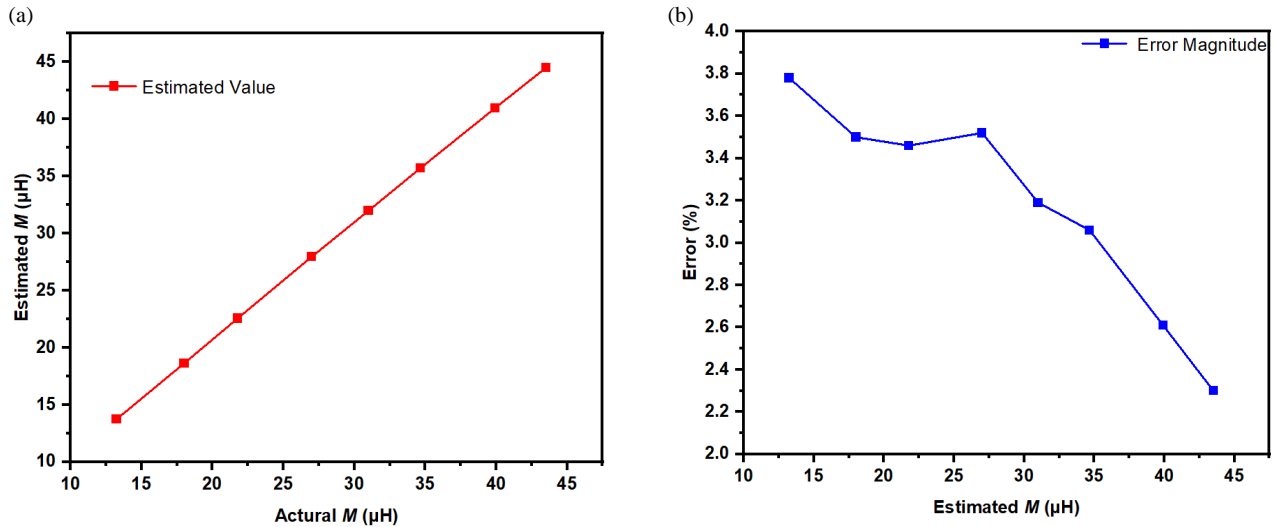


FIGURE 9. Mutual inductance estimation value and real value. (a) Mutual inductance estimation curve. (b) Estimation error curve.

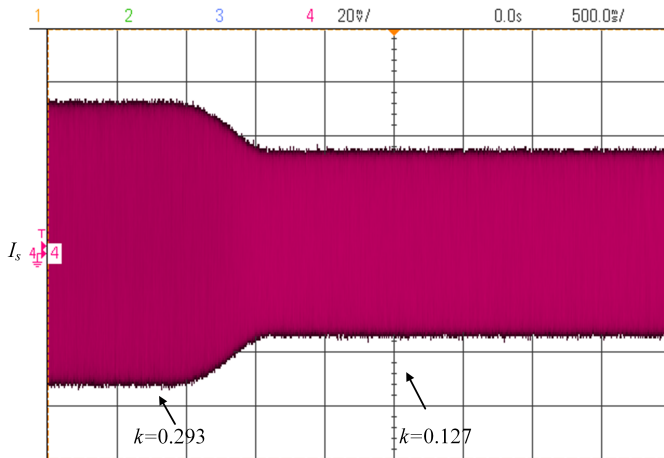


FIGURE 10. Current I_s waveform.

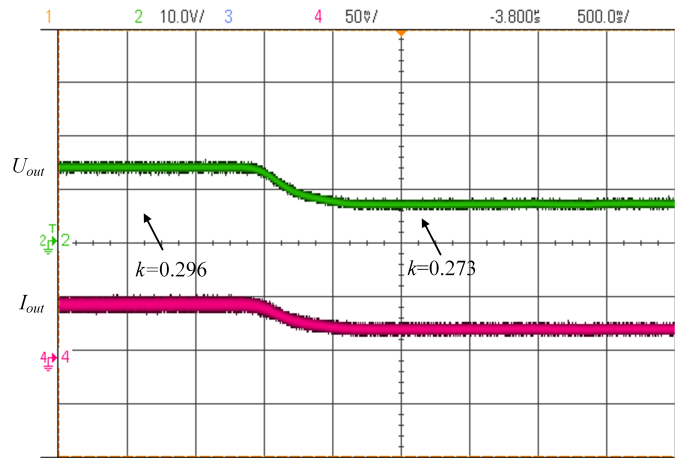


FIGURE 11. Changes of load voltage and current.

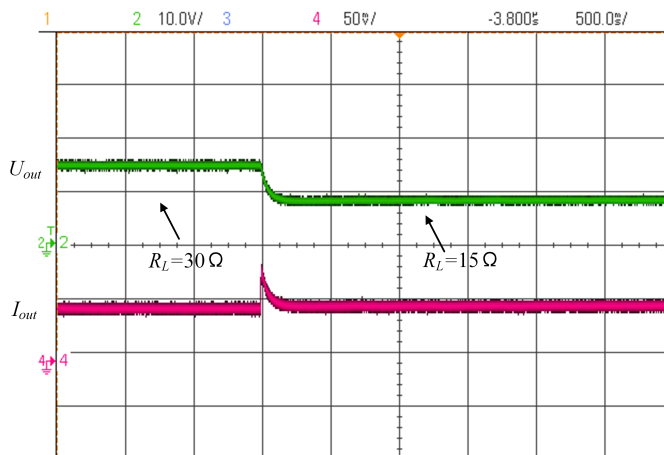


FIGURE 12. MEPT when the load changes.

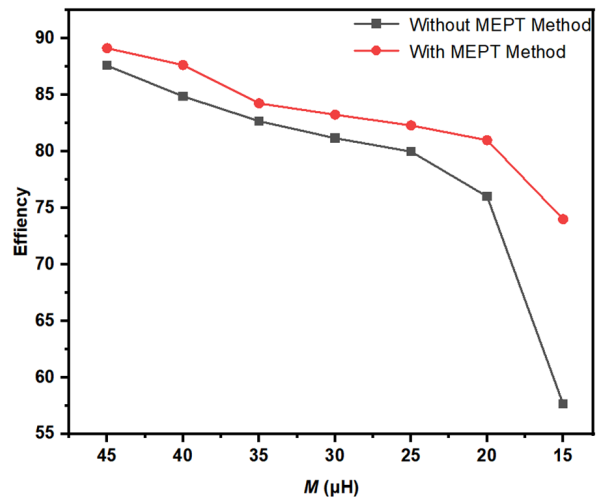


FIGURE 13. System transmission efficiency comparison.

inductance between the coils decreases, that is, the coupling coefficient changes from 0.296 to 0.273, and the system load output decreases. Through the proposed MEPT method, the system efficiency can be maintained at the optimal level.

For the load disturbance, the coil position is fixed in this paper, that is, the system coupling coefficient is kept at $k = 0.3$, and the load R_L is changed from $30\ \Omega$ to $15\ \Omega$. The system load voltage U_{out} and current I_{out} are collected, and the voltage and current change waveforms are shown in Fig. 12. It can be seen from Fig. 12 that as the load changes, the duty cycle is changed in real time by the proposed method to maximize the system output efficiency.

Figure 13 shows the efficiency curves of the WPT system with or without MEPT control method when the load $R_L = 30$, where the red line indicates the efficiency without MEPT control method, and the black line indicates the efficiency with MEPT control method. It can be seen from Fig. 13 that the transmission efficiency of the WPT system has been greatly improved after using the maximum efficiency tracking method based on dynamic coupling coefficient estimation proposed in this paper. This situation is particularly obvious in the case of large-scale offset, that is, when the mutual inductance is $13.5\ \mu\text{H}$, the system efficiency is improved by 17%. In the whole migration process, the system efficiency is always maintained at more than 72%.

5. CONCLUSION

In order to enhance the anti-offset ability of underwater wireless power transmission system and improve the transmission efficiency of the system, this paper proposes a maximum efficiency tracking of underwater wireless power transmission system based on dynamic coupling coefficient estimation. By using the known attempt of the system and the effective value of the current flowing through the receiving coil on the receiving side, the dynamic parameter identification of mutual inductance is realized without communication. On this basis, the identification results are used for impedance matching, so as to improve the system efficiency. The theoretical method studied in this paper is verified by experiments. The experimental results show that the parameter identification method proposed in this paper can accurately estimate the mutual inductance value, and the efficiency of the system is 18% higher than that without maximum efficiency control when the system is shifted in a large range. The effectiveness of the method is verified by experiments. Due to the limited experimental equipment, the array arrangement will be used for large-scale migration in the future.

REFERENCES

- [1] Zhou, H., J. Chen, Q. Deng, F. Chen, A. Zhu, W. Hu, and X. Gao, "Input-series output-equivalent-parallel multi-inverter system for high-voltage and high-power wireless power transfer," *IEEE Transactions on Power Electronics*, Vol. 36, No. 1, 228–238, Jan. 2021.
- [2] Lai, K.-T., F.-C. Cheng, S.-C. T. Chou, Y.-C. Chang, G.-W. Wu, and J.-C. Tsai, "AnyCharge: An IoT-based wireless charging service for the public," *IEEE Internet of Things Journal*, Vol. 6, No. 6, 10 888–10 901, Dec. 2019.
- [3] Li, Y., K. Xie, and Y. Ying, "A novel magnetic coupler with low leakage EMF for AUV wireless power transfer system," *IEEE Journal of Emerging and Selected Topics in Industrial Electronics*, Vol. 5, No. 1, 212–224, Jan. 2024.
- [4] Wang, L., P. Sun, Y. Liang, L. He, X. Wu, and Q. Deng, "Research on the control strategy of communication-free IPT system based on multi-parameter joint real-time identification," *IEEE Transactions on Power Electronics*, Vol. 39, No. 1, 1912–1926, Jan. 2024.
- [5] Yang, L., Y. Zhang, X. Li, B. Feng, X. Chen, J. Huang, T. Yang, D. Zhu, A. Zhang, and X. Tong, "Comparison survey of effects of hull on AUVs for underwater capacitive wireless power transfer system and underwater inductive wireless power transfer system," *IEEE Access*, Vol. 10, 125 401–125 410, 2022.
- [6] Anyapo, C. and P. Intani, "Wireless power transfer for autonomous underwater vehicle," in *2020 IEEE PELS Workshop on Emerging Technologies: Wireless Power Transfer (WoW)*, 246–249, Seoul, Korea (South), 2020.
- [7] Bhargavi, K. M., K. A. Manohar, B. S. Sagarika, P. L. Sharanya, and C. R. Lohith, "Wireless power transmission of electric vehicle," in *2023 International Conference on Network, Multimedia and Information Technology (NMITCON)*, 1–5, Bengaluru, India, 2023.
- [8] Wang, Z.-H., Y.-P. Li, Y. Sun, C.-S. Tang, and X. Lv, "Load detection model of voltage-fed inductive power transfer system," *IEEE Transactions on Power Electronics*, Vol. 28, No. 11, 5233–5243, Nov. 2013.
- [9] Su, Y.-G., L. Chen, X.-Y. Wu, A. P. Hu, C.-S. Tang, and X. Dai, "Load and mutual inductance identification from the primary side of inductive power transfer system with parallel-tuned secondary power pickup," *IEEE Transactions on Power Electronics*, Vol. 33, No. 11, 9952–9962, Nov. 2018.
- [10] Yin, J., D. Lin, T. Parisini, and S. Y. Hui, "Front-end monitoring of the mutual inductance and load resistance in a series-series compensated wireless power transfer system," *IEEE Transactions on Power Electronics*, Vol. 31, No. 10, 7339–7352, Oct. 2016.
- [11] Yeo, T.-D., D. Kwon, S.-T. Khang, and J.-W. Yu, "Design of maximum efficiency tracking control scheme for closed-loop wireless power charging system employing series resonant tank," *IEEE Transactions on Power Electronics*, Vol. 32, No. 1, 471–478, Jan. 2017.
- [12] Hu, J., J. Zhao, and C. Cui, "A wide charging range wireless power transfer control system with harmonic current to estimate the coupling coefficient," *IEEE Transactions on Power Electronics*, Vol. 36, No. 5, 5082–5094, May 2021.
- [13] Ikeda, K., T. Imura, and Y. Hori, "Maximum efficiency control on the receiving side using LCC-LCC compensation topology for dynamic wireless power transfer," in *IECON 2023 — 49th Annual Conference of the IEEE Industrial Electronics Society*, 1–6, Singapore, Singapore, 2023.
- [14] Orekan, T., P. Zhang, and C. Shih, "Analysis, design, and maximum power-efficiency tracking for undersea wireless power transfer," *IEEE Journal of Emerging and Selected Topics in Power Electronics*, Vol. 6, No. 2, 843–854, Jun. 2018.
- [15] Jiwariyavej, V., T. Imura, and Y. Hori, "Coupling coefficients estimation of wireless power transfer system via magnetic resonance coupling using information from either side of the system," *IEEE Journal of Emerging and Selected Topics in Power Electronics*, Vol. 3, No. 1, 191–200, Mar. 2015.
- [16] Zhuo, H., J. Xiao, W. Gong, X. Zhang, and Y. Chang, "Research on transmission characteristics of MCR-WPT systems based on

- chaotic sparrow search algorithm,” in *2023 IEEE International Conference on Power Science and Technology (ICPST)*, 1064–1069, Kunming, China, 2023.
- [17] Hu, J., J. Zhao, and F. Gao, “A real-time maximum efficiency tracking for wireless power transfer systems based on harmonic-informatization,” *IEEE Transactions on Power Electronics*, Vol. 38, No. 1, 1275–1287, Jan. 2023.
- [18] Yang, J., Y. Liu, K. Yue, Z. Guan, M. Fu, and H. Wang, “Closed-form solutions of mutual inductance and load for LCC-S wireless power transfer systems,” in *2023 IEEE 3rd International Conference on Industrial Electronics for Sustainable Energy Systems (IESES)*, 1–6, Shanghai, China, 2023.
- [19] Wang, L., P. Sun, Y. Liang, J. Sun, X. Wu, H. Shen, and Q. Deng, “Joint real-time identification for mutual inductance and load charging parameters of IPT system,” *IEEE Journal of Emerging and Selected Topics in Power Electronics*, Vol. 11, No. 4, 4574–4590, Aug. 2023.
- [20] Jin, R., Z. Yang, and F. Lin, “Mutual inductance identification and maximum efficiency control of wireless power transfer system for the modern tram,” in *2017 IEEE PELS Workshop on Emerging Technologies: Wireless Power Transfer (WoW)*, 70–74, Chongqing, China, 2017.
- [21] Yamada, Y., T. Imura, and Y. Hori, “A method for determining resonant elements considering the requirements of double-LCC circuits in dynamic wireless power transfer,” in *2022 Wireless Power Week (WPW)*, 766–771, Bordeaux, France, 2022.
- [22] Esfahani, F. N., S. M. Madani, M. Niroomand, and A. Safaei, “Maximum wireless power transmission using real-time single iteration adaptive impedance matching,” *IEEE Transactions on Circuits and Systems I: Regular Papers*, Vol. 70, No. 9, 3806–3817, Sep. 2023.